Interference-Aware Multi-Iterative Equalization and Detection for Frequency-Selective MIMO Channels

Tobias Seifert, Xiaohang Song and Gerhard Fettweis
Vodafone Chair Mobile Communications Systems
Technische Universität Dresden
Dresden, Germany
Email: {tobias.seifert, xiaohang.song, fettweis}@ifn.et.tu-dresden.de

***Abstract*—Turbo equalization has demonstrated to be a powerful approach for wireless transmission over frequency-selective channels introducing intersymbol interferences (ISI). Regarding multiple-input multiple-output (MIMO) systems, tree-search based MIMO detection techniques (e.g., sphere detection) are well suited for significantly reducing multi-antenna interferences. However, direct application of these detection techniques under the presence of ISI leads to vast processing complexity, increasing exponentially with the channel length and the number of transmitting antennas. In this paper, a low-complex two-stage approach is described splitting the interference reduction into a frequency-domain equalization stage and a time-domain sphere detection stage. Both are able to take a-priori information into account. Based on this, we derive a novel multi-iterative receiver, enabling powerful and adaptable processing with respect to the dominating interferences.**

I. Introduction

Modern and future mobile communication generations, like long term evolution (LTE) advanced [1], make use of multiple-input multiple-output (MIMO) techniques to fulfill the ever-increasing demand on high spectral efficiency. These techniques require a MIMO detector at the receiver side in order to deal with appearing inter-antenna interferences (IAI). In this regard, tree-search based detection algorithms, particularly soft-output sphere detection, have shown to provide error-rate performance close to *maximum a-posteriori probability* detection performance at comparatively low complexity [2]. Considering coded transmission, the detection result can further be improved by taking a-priori information (provided by the decoder) into account. The basis for that is a soft-input soft-output (SISO) sphere detector [3], which can be efficiently implemented in hardware [4], [5].

However, since the complexity of a tree search increases exponentially with the number of channel taps, high-throughput sphere detection is only possible if frequency-flat MIMO channels are considered, having a discrete channel impulse response of length one. While this condition holds for the LTE downlink, multipath propagation in the uplink causes intersymbol interference (ISI) as a consequence of the deployed single-carrier frequency-divison multiple access (SC-FDMA) transmission scheme. This interference corrupts the received signal in addition to the present IAI.

In order to still apply tree-search based detection to frequency-selective MIMO channels, a two-stage approach has been introduced in [6], where the equalizer in the first stage is deployed to reduce the number of channel taps. The subsequent MIMO detector processes a dimension-reduced channel matrix, leading to a more reliable output compared to linear equalization. Similar to SISO sphere detectors, equalizers in single-antenna systems can benefit from coded transmission by performing block-based equalization-decoding iterations, known as turbo equalization [7]. This concept has been extended to multiple-antenna systems, as done in [8], [9]. Unfortunately, these solutions are single-stage schemes, jointly equalizing ISI and IAI in the frequency-domain. Hence, they do not allow for powerful IAI cancellation by means of time-domain tree-search detection.

This paper presents a novel multi-iterative receiver based on a two-stage equalization-detection scheme. The key component is a SISO frequency-domain equalization (FDE) that shortens the impulse responses of the frequency-selective channels. This equalizer comprises essentially an adaptive minimum mean square error (MMSE) filter matrix which is (in combination with a feedback signal vector) able to take a-priori information into account. Afterwards, a SISO sphere detector is involved to achieve low error-rates, especially in high-order antenna systems. The proposed two-stage scheme is analyzed in terms of frame error-rate (FER) performance and compared to a conventional scheme using only a single-stage SISO FDE. The paper completes with an investigation of the relative number of necessary iteration runs when a stop criterion is applied. Based on this, the FER performance in high-ISI MIMO channels can be improved by $2\,\mathrm{dB}$ at the cost of increased complexity by a factor of 1.6.

II. System Model for the LTE-A Uplink

Throughout this paper we consider an LTE-A uplink transmission scenario based on SC-FDMA with T transmitting and R receiving antennas, as depicted in Fig. 1. Each transmit layer $t = 1, ..., T$ may correspond to a different user, for which reason the transmit processing steps are carried out individually for each stream.

The encoder of the t-th transmit layer converts a binary source vector (transport block) $\mathbf{u}_t$ into an encoded vector $\mathbf{c}_t$ with code rate ρ. To ensure proper accomodation of the transmitted signal to the available resources, the encoder also performs puncturing or repetition of bits. The vector $\mathbf{c}_t$ is

978-1-4799-6664-6/16/$31.00 ©2016 IEEE

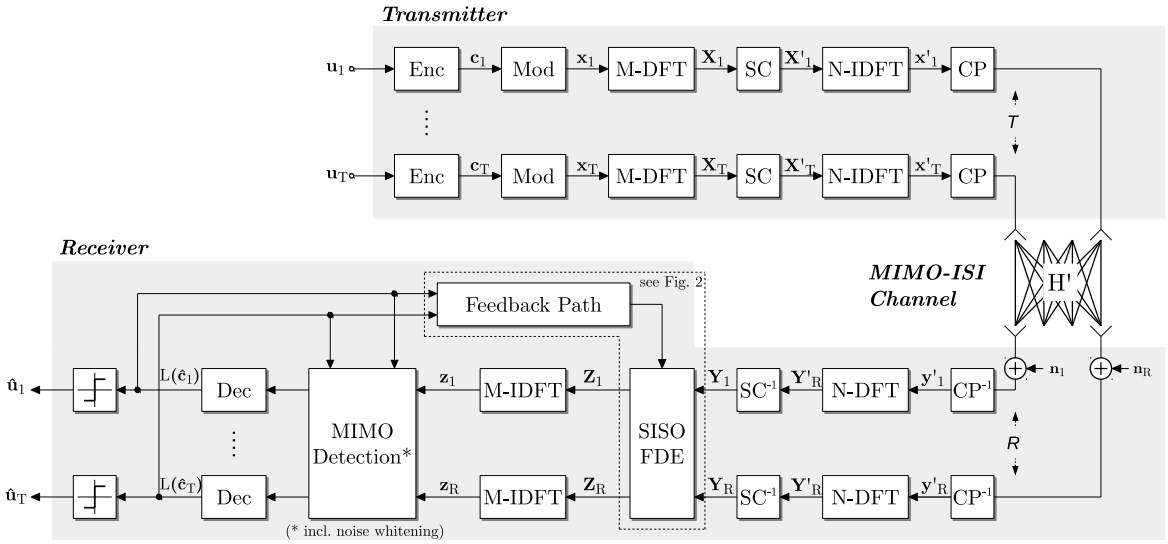

Fig. 1. System model of the LTE-A uplink scenario for the generic MIMO case. The receiver comprises a two-stage equalization-detection scheme.

modulated by mapping μ bits to a corresponding 2^μ-QAM symbol $x_t[m]$ at time instant m. Note that the transmit power at each transmitting antenna is assumed to be unitary, i.e., $\mathrm{E}[|x_t[m]|^2] = \sigma_x^2 = 1$.

M consecutive symbols are combined to a SC-FDMA symbol $\mathbf{x}_t = [x_t[1], ..., x_t[M]]^{\mathrm{T}}$, where $(\cdot)^{\mathrm{T}}$ denotes the transpose operation. $\mathbf{x}_t$ is serial-to-parallel converted and subsequently transformed to frequency-domain by an M-point DFT. The frequency components are mapped to $N > M$ contiguous subcarriers such that frequency resources can be shared with other users. This subcarrier mapping can be represented by a matrix $\mathbf{D} \in \{0,1\}^{N \times M}$ with ones corresponding to the allocated frequencies and zeros otherwise. An N-point inverse DFT returns the serialized transmit SC-FDMA signal vector

$$\mathbf{x}'_t = \mathbf{F}_N^{\mathrm{H}} \mathbf{D} \mathbf{F}_M \mathbf{x}_t, \tag{1}$$

where $(\cdot)^{\mathrm{H}}$ denotes the Hermitian operator and $\mathbf{F}_M \in \mathbb{C}^{M \times M}$ is the Fourier matrix of an M-point DFT. Finally, a cyclic prefix (CP) is added to each t-th transmit signal $\mathbf{x}'_t$, preventing interferences between successive SC-FDMA symbols and turning the linear convolution between the channel impulse response and the transmit signal into a circular convolution. This enables efficient FDE on the receiver side since all subcarriers are decoupled [10], [11]. Note that instead of using a CP in the model, the subchannel matrix $\mathbf{H}'_{r,t}$ itself is assumed to be circular to remain circular property in the transmission.

Stacking up the outputs of all transmitting antennas, the received SC-FDMA signal vector $\mathbf{y}' \in \mathbb{C}^{RN \times 1}$ is given by

$$\begin{bmatrix} \mathbf{y}'_1 \\ \vdots \\ \mathbf{y}'_R \end{bmatrix} = \begin{bmatrix} \mathbf{H}'_{1,1} & \cdots & \mathbf{H}'_{1,T} \\ \vdots & \ddots & \vdots \\ \mathbf{H}'_{R,1} & \cdots & \mathbf{H}'_{R,T} \end{bmatrix} \begin{bmatrix} \mathbf{x}'_1 \\ \vdots \\ \mathbf{x}'_T \end{bmatrix} + \begin{bmatrix} \mathbf{n}'_1 \\ \vdots \\ \mathbf{n}'_R \end{bmatrix}, \tag{2}$$

where $\mathbf{n}'_r$ is a complex-valued white Gaussian noise vector $\mathbf{n}'_r \sim \mathcal{CN}(\mathbf{0}, \sigma_{\mathrm{n}}^2 \mathbf{I}_N)$. Each subchannel matrix $\mathbf{H}'_{r,t} \in \mathbb{C}^{N \times N}$ represents the considered frequency-selective channel between transmitting antenna t and receiving antenna r. Taking the circular property into account, $\mathbf{H}'_{r,t}$ is a Toeplitz matrix and has the format

$$\mathbf{H}'_{r,t} = \begin{bmatrix} h'_{r,t}[1] & h'_{r,t}[N] & \dots & h'_{r,t}[3] & h'_{r,t}[2] \\ h'_{r,t}[2] & h'_{r,t}[1] & \dots & h'_{r,t}[4] & h'_{r,t}[3] \\ \vdots & \ddots & \ddots & \ddots & \vdots \\ h'_{r,t}[N] & h'_{r,t}[N-1] & \dots & h'_{r,t}[2] & h'_{r,t}[1] \end{bmatrix}. \tag{3}$$

Each column corresponds to a (circular shifted) subchannel impulse response $\mathbf{h}'_{r,t} = [h'_{r,t}[1], ..., h'_{r,t}[N]]^{\mathrm{T}}$ where only the first $L \leq N$ entries are non-zero values. The subchannel coefficients $h'_{r,t}[n]$ are realizations of a zero-mean i.i.d. Gaussian random process with weighted variances according to a given power delay profile (PDP). The total channel power is normalized with respect to the number of transmitting antennas, resulting $\sum_{n=1}^{L} \mathrm{E}[|h'_{r,t}[n]|^2] = 1/T$. After the N-point DFT and the subcarrier demapping, the relation between the transmitted and received signal in the frequency-domain is given by

$$\begin{bmatrix} \mathbf{Y}_1 \\ \vdots \\ \mathbf{Y}_R \end{bmatrix} = \begin{bmatrix} \mathbf{H}_{1,1} & \cdots & \mathbf{H}_{1,T} \\ \vdots & \ddots & \vdots \\ \mathbf{H}_{R,1} & \cdots & \mathbf{H}_{R,T} \end{bmatrix} \begin{bmatrix} \mathbf{X}_1 \\ \vdots \\ \mathbf{X}_T \end{bmatrix} + \begin{bmatrix} \mathbf{N}_1 \\ \vdots \\ \mathbf{N}_R \end{bmatrix}, \tag{4}$$

Due to the circular property of $\mathbf{H}'_{r,t}$, each submatrix

$$\mathbf{H}_{r,t} = \mathbf{D}^{\mathrm{T}} \mathbf{F}_N \mathbf{H}'_{r,t} \mathbf{F}_N^{\mathrm{H}} \mathbf{D} \tag{5}$$

is an $M \times M$ diagonal matrix and can be considered as the effective frequency-domain subchannel matrix. There is still spatial correlation between signals transmitted by different antennas but no more coupling between signals transmitted at different subcarriers.

The SISO FDE processes the received vector $\mathbf{Y} \in \mathbb{C}^{RM \times 1}$ in consideration of a-priori knowledge and outputs the equalized vector $\mathbf{Z} \in \mathbb{C}^{RM \times 1}$. Details concerning SISO FDE or

feedback path of the receiver are presented in Section IV. After an M-point IDFT, the time-domain symbol vector $\mathbf{z}$ passes a MIMO detection unit. This detector unit resolves remaining interference IAI and determines log-likelihood-ratio (LLR) values $L(\hat{\mathbf{c}}'_t)$, subsequently passed to a decoder. The decoder's soft-output $L(\hat{\mathbf{c}}_t)$ may be fed back to the equalizer and/or the MIMO detector to benefit from turbo principle [12], increasing the reliability of the final estimates $\hat{\mathbf{u}}_t$. Note that depending on the available subcarriers M, an encoded transport block $\mathbf{c}_t$ can comprise multiple SC-FDMA symbols.

III. Single-Stage Frequency-Domain Equalization

Linear FDE is an often used approach to equalize received signals which are, additionally to IAI, impaired by ISI. Due to the CP in SC-FDMA, the equalization can be carried out independently for all M subcarriers, resulting in M different filter matrices $\mathbf{C}[m] \in \mathbb{C}^{T\times R}$. When applying the MMSE criterion to the system model in Fig. 1 and assuming that no feedback path is present, the linear FDE filter for the m-th subcarrier is given by the well known MMSE filter as

$$\mathbf{C}_{\text{MMSE}}[m] = \mathbf{H}^{\text{H}}[m]\big(\mathbf{H}[m]\mathbf{H}^{\text{H}}[m] + \sigma_{\text{n}}^2\mathbf{I}_T\big)^{-1}, \qquad (6)$$

where $\mathbf{H}[m] \in \mathbb{C}^{R\times T}$ denotes the frequency-domain MIMO channel for subcarrier m, composed of the corresponding m-th diagonal elements of the matrices $\mathbf{H}_{r,t}$, i.e.,

$$\mathbf{H}[m] = \begin{bmatrix} \big(\mathbf{H}_{1,1}\big)_{m,m} & \dots & \big(\mathbf{H}_{1,T}\big)_{m,m} \\ \vdots & \ddots & \vdots \\ \big(\mathbf{H}_{R,1}\big)_{m,m} & \dots & \big(\mathbf{H}_{R,T}\big)_{m,m} \end{bmatrix}. \qquad (7)$$

Since ISI and IAI are jointly equalized within a single-stage, the MIMO detector reduces to T independent soft-demodulators.

Linear FDE allows low computational complex receiver implementations, but the equalized signal vector $\mathbf{Z}$ retains significant interference that leads to low communication performance. Performing block-based iterative equalization-decoding can provide significant performance gains [7]. Hence, the soft-output FDE in (6) has been extended to a SISO FDE that combines adaptive MMSE filtering with additional parallel interference cancellation [8], [9].

IV. Multi-Iterative Two-Stage Equalization and Detection

Frequency-selective MIMO channels typically do not allow the application of sophisticated MIMO detection techniques (like tree-search based detection) since the computational complexity increases exponentially with length L of the sub-channel impulse responses. In order to still use these detection techniques at reasonable complexity, an FDE is deployed to shorten L before carrying out tree-search based detection in a dimension-reduced MIMO system [6]. This results in a two-stage approach well suited for implementation since the complexity is now independent of L.

Although a proper distinction between interference parts caused by temporal and those caused by spatial correlation is not possible, the two-stage equalization and detection method can be interpreted as an *ISI cancellation* step (performed by the FDE) followed by an *IAI cancellation* step (performed by the MIMO detector). For this purpose, a new ISI-free target channel matrix $\tilde{\mathbf{H}}$ is introduced. Its subchannel matrices are given by

$$\tilde{\mathbf{H}}_{r,t} = h'_{r,t}[1]\mathbf{I}_M, \qquad (8)$$

taking only the first and most often dominating channel tap into account. Since $\tilde{\mathbf{H}}_{r,t}$ is a scaled identity matrix, no distinction between frequency- and time-domain representation is necessary, i.e., $\tilde{\mathbf{H}}_{r,t} = \mathbf{F}_M\tilde{\mathbf{H}}_{r,t}\mathbf{F}_M^{\text{H}}$. Figure 3 shows an analysis of two channel power profiles under different ISI levels.

Within this Section we develop a SISO FDE for the two-stage equalization-detection approach. This allows the application of turbo equalization mechanism (similar as used for the single-stage approach) which can additionally be combined with iterative detection-decoding. The resulting receiver structure has multiple feedback paths, as shown in Fig. 1, enabling flexible multi-iterative receiver processing depending on the channel conditions.

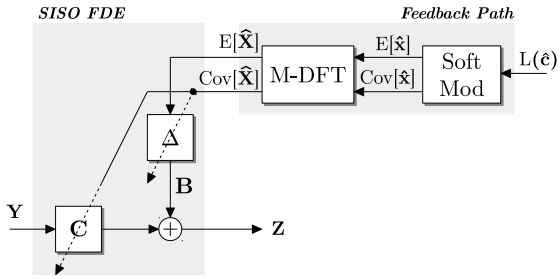

Fig. 2. Detailed structure of the feedback path and the SISO FDE depicted in the receiver of Fig. 1. The dashed line indicates that $\text{Cov}[\hat{\mathbf{X}}]$ adapts filter $\mathbf{C}$ and Δ.

A. Structure of SISO FDE

The detailed structure of the SISO FDE as well as the feedback path is depicted in Fig. 2. It is assumed that $\mathbf{Y}$ is first multiplied by a filter matrix $\mathbf{C}$ and subsequently added to an ISI feedback signal $\mathbf{B}$, resulting in the equalizer output

$$\mathbf{Z} = \mathbf{C}\mathbf{Y} + \mathbf{B}. \qquad (9)$$

Note that at this point no further assumption on the specific functionality of the feedback path is necessary.

B. Design of Feedforward Filter and ISI Feedback Signal

Considering Equation (5), the overall effective frequency-domain channel matrix $\mathbf{H} \in \mathbb{C}^{RM\times TM}$ can be described by

$$\mathbf{H} = \big(\mathbf{I}_R \otimes \mathbf{D}^{\text{T}}\big)\underbrace{\big(\mathbf{I}_R \otimes \mathbf{F}_N\big)}_{\underline{\mathbf{F}}_{RN}}\mathbf{H}'\underbrace{\big(\mathbf{I}_T \otimes \mathbf{F}_N^{\text{H}}\big)}_{\underline{\mathbf{F}}_{TN}^{\text{H}}}\big(\mathbf{I}_T \otimes \mathbf{D}\big) \qquad (10)$$

where $\otimes$ denotes the kronecker product. When performed between an identity matrix of size T and a Fourier matrix

of size M, its short form is defined by $\underline{\mathbf{F}}_{TM}$. Taking the ISI-free channel matrix $\tilde{\mathbf{H}}$ into account and applying the MMSE criterion, a cost function J at the output of the M-IDFTs can be expressed as

$$\begin{aligned} J &= \mathrm{E}\left[\left\|\mathbf{z}-\tilde{\mathbf{H}}\mathbf{x}\right\|^2\right] \\ &= \mathrm{E}\left[\left\|\underline{\mathbf{F}}_{RM}^{\mathrm{H}}\big(\mathbf{Z}-\tilde{\mathbf{H}}\underline{\mathbf{F}}_{TM}\underbrace{\underline{\mathbf{F}}_{TM}^{\mathrm{H}}\mathbf{X}}_{\mathbf{x}}\big)\right\|^2\right]. \end{aligned} \tag{11}$$

Inserting (9) into (11) and using (4) leads to

$$J = \mathrm{E}\left[\left\|\underline{\mathbf{F}}_{RM}^{\mathrm{H}}\left(\mathbf{B}+\mathbf{C}\mathbf{H}\mathbf{X}+\mathbf{C}\mathbf{N}-\tilde{\mathbf{H}}\mathbf{X}\right)\right\|^2\right], \tag{12}$$

which needs to be minimized. The time-domain transmit symbol vector $\mathbf{x}$ is a random variable, whose mean and covariance can be derived from soft-bits (LLR values) determined in a previous iteration [13]. For the given receiver description, the feedback path in Fig. 2 transforms the decoder output $L(\hat{\mathbf{c}})$ into frequency-domain soft-symbols (given by $\mathrm{E}[\hat{\mathbf{X}}]$ and $\mathrm{Cov}[\hat{\mathbf{X}}]$), representing an a-priori information for the SISO FDE.

The ISI feedback signal $\mathbf{B}$ is calculated by setting the complex-valued derivative to zero, i.e., $\partial J/\partial \mathbf{B}^{\mathrm{H}} = 0$, resulting in

$$\mathbf{B} = \left(\tilde{\mathbf{H}}-\mathbf{C}\mathbf{H}\right)\mathrm{E}\left[\hat{\mathbf{X}}\right]. \tag{13}$$

For the derivation of the feedforward filter matrix $\mathbf{C}$, it is assumed that $\mathrm{E}[\mathbf{X}\mathbf{N}^{\mathrm{H}}] = \mathbf{0}$. Inserting (13) in (12) and performing partial derivation $\partial J/\partial \mathbf{C}^{\mathrm{H}} = 0$, the filter matrix is obtained as

$$\mathbf{C} = \tilde{\mathbf{H}}\,\mathrm{Cov}\left[\hat{\mathbf{X}}\right]\mathbf{H}^{\mathrm{H}}\Big(\mathbf{H}\,\mathrm{Cov}\left[\hat{\mathbf{X}}\right]\mathbf{H}^{\mathrm{H}}+\mathrm{Cov}\left[\mathbf{N}\right]\Big)^{-1}, \tag{14}$$

with frequency-domain covariance matrices given by

$$\mathrm{Cov}\Big[\hat{\mathbf{X}}\Big] = \underline{\mathbf{F}}_{TM}\,\mathrm{Cov}\left[\hat{\mathbf{x}}\right]\underline{\mathbf{F}}_{TM}^{\mathrm{H}} \quad \text{and} \tag{15}$$

$$\mathrm{Cov}\Big[\mathbf{N}\Big] = \sigma_{\mathrm{n}}^2\mathbf{I}_{RM}. \tag{16}$$

In the initial receiving process (*0th iteration*), when no a-priori information is available, the soft-input for the equalizer is set to $\mathrm{Cov}[\hat{\mathbf{X}}] = \mathbf{I}_{TM}$, turning $\mathbf{C}$ into the adapted MMSE filter $\tilde{\mathbf{H}}\mathbf{C}_{\mathrm{MMSE}}$ and $\mathbf{B}$ to zero. The other extreme is the presence of highly reliable estimates, i.e., $\mathrm{Cov}[\hat{\mathbf{X}}] \approx \mathbf{0}$. In this feedback scenario, filter $\mathbf{C} = \mathbf{0}$ blocks $\mathbf{Y}$ and the equalizer outputs $\mathbf{B} = \tilde{\mathbf{H}}\,\mathrm{E}[\hat{\mathbf{X}}]$, which is the same output as in the previous iteration. This corner case explains the observed performance saturation later shown in Section V.

C. Computational Complexity Reduction

The calculation of filter matrix $\mathbf{C} \in \mathbb{C}^{RM\times RM}$ implies very high complexity, especially regarding the necessary matrix inversion operation. However, since the entries $\mathrm{Var}[\hat{x}_{t,m}]$ of the diagonal time-domain covariance matrix $\mathrm{Cov}[\hat{\mathbf{x}}_t]$ hardly scatter for a given signal-to-noise ratio (SNR) value, the corresponding frequency-domain covariance matrix can be approximated by its diagonal, leading to

$$\mathrm{Cov}\left[\hat{\mathbf{X}}_t\right] \approx \mathrm{diag}\Big\{\mathrm{Cov}\left[\hat{\mathbf{X}}_t\right]\Big\} = \sigma_{\hat{X}_t}^2\mathbf{I}_M, \tag{17}$$

with $\sigma_{\hat{X}_t}^2 = {}^1\!/_M \sum_{m=1}^{M}\mathrm{Var}\left[\hat{x}_{t,m}\right]$. Note that all cross-covariance matrices $\mathrm{Cov}[\hat{\mathbf{X}}_{t_1}\hat{\mathbf{X}}_{t_2}]$ with $t_1 \neq t_2$ are zero if the transmitting antennas are uncorrelated. Applying the approximation and using the matrix inversion lemma, (14) can be decomposed in M filter matrices

$$\mathbf{C}[m] = \tilde{\mathbf{H}}[m]\Big(\mathbf{H}^{\mathrm{H}}[m]\mathbf{H}[m]+\sigma_{\mathrm{n}}^2\,\mathrm{Cov}^{-1}[\hat{\mathbf{X}}[m]]\Big)^{-1}\mathbf{H}^{\mathrm{H}}[m] \tag{18}$$

of size $R\times R$, resulting in similar complexity as (6). Both $\tilde{\mathbf{H}}[m]$ and $\mathrm{Cov}^{-1}[\hat{\mathbf{X}}[m]]$ are independent of m.

D. Noise Whitening and MIMO Detection

The main idea behind the two-stage approach is to cancel the residual antenna interference by means of a separate MIMO detector which mostly assumes spatially uncorrelated noise samples with covariance matrix $\sigma_{\mathrm{n}}^2\mathbf{I}_T$. However, a side effect of the previous equalization step is that it introduces correlation (colored noise). Hence, the noise in the time-domain SISO FDE output $\mathbf{z}$ needs to be whitened.

A noise whitening filter (NWF) can be derived from the noise covariance matrix present at the NWF input, given by

$$\mathrm{Cov}[\mathbf{n}_{\mathrm{c}}] = \mathrm{Cov}[\underline{\mathbf{F}}_{RM}^{\mathrm{H}}\mathbf{C}\mathbf{N}] = \sigma_{\mathrm{n}}^2\underbrace{\mathbf{C}'\mathbf{C}'^{\mathrm{H}}}_{\mathbf{W}}, \tag{19}$$

where $\mathbf{C}' = \underline{\mathbf{F}}_{RM}^{\mathrm{H}}\mathbf{C}\underline{\mathbf{F}}_{RM}$ denotes the time-domain equivalent SISO FDE filter matrix. Whitening is done by multiplying $\mathbf{z}$ by $\mathbf{W}^{-1/2}$. The NWF output is now given by

$$\mathbf{z}_{\mathrm{w}} = \underbrace{\mathbf{W}^{-1/2}\tilde{\mathbf{H}}}_{\mathbf{\Phi}}\mathbf{x} + \mathbf{W}^{-1/2}\mathbf{n}_{\mathrm{c}}. \tag{20}$$

Each $\mathbf{z}_{\mathrm{w}}[m]$ is an effective received symbol vector of $\mathbf{x}[m]$ transmitted over a flat $R\times T$ MIMO channel $\mathbf{\Phi}[m]$. Note that $\mathbf{\Phi}[m]$ is identical for all m.

Due to the shortened channel length, the MIMO detection can be carried out by nonlinear detection techniques using search trees.

As depicted in Fig. 1 both stages, the SISO FDE and the MIMO detector, can process a-priori information. In order to fully benefit from turbo principle, two feedback paths must be present in the receiver, connecting the decoder with the SISO FDE and the MIMO detector separately. Hence in an iteration loop, the MIMO detector does not only take a-priori values from the turbo decoder but also further ISI-reduced inputs from the SISO FDE to improve the detection result.

V. Communications Performance and Iterations Complexity

The iterative two-stage equalization-detection scheme introduced in the previous chapter is compared to the single-stage SISO FDE in terms of FER performance. For this purpose two channel scenarios with different power delay profiles

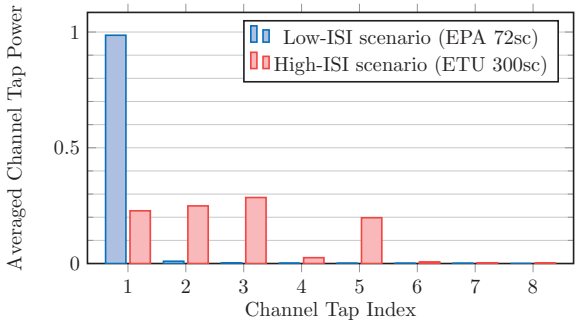

Fig. 3. Resulting channel tap power profiles for two different channel scenarios. The low-ISI scenario is represented by using the *extended pedestrian A (EPA)* model with 1.4 MHz user bandwidth (72 subcarriers). The high-ISI scenario is represented by using the *extended typical urban (ETU)* model with 5.0 MHz user bandwidth (300 subcarriers).

and different user bandwidths are considered and defined as follows:

- Low-ISI scenario: Extended pedestrian A (EPA) model with 1.4 MHz ($M = 72$ subcarriers)
- High-ISI scenario: Extended typical urban (ETU) model with 5.0 MHz ($M = 300$ subcarriers)

The power profiles of the corresponding discrete channel impulse responses $h'[n]$ are depicted in Fig. 3. While the high-ISI scenario results in 5 channel taps, the low-ISI leads to an almost frequency-flat channel. As illustrated, the first channel tap $h'[1]$ of the high-ISI case is not the most dominant one but still big enough for being used for the composition of the target MIMO channel matrix in (8).

The comparative analysis of FER performance in the LTE-A uplink is shown in Fig. 4. For all scenarios a 4×4 MIMO system with channel quality indicator (CQI) of 10 is selected, resulting in transmission of 64-QAM constellation symbols at turbo code rate $\rho = 0.45$. At the receiver side, a tuple search sphere detector (TSD) with predefined search sequences is used [14]. Its tree search complexity is constraint by a maximum tuple size of 16 elements. Note that the TSD only produces soft-outputs but is not capable to process soft-inputs. Therefore the decoder in Fig. 1 exhibits only a feedback connection to the SISO FDE, but not to the MIMO detector. This allows to carry out a predefined number of *#It* equalization-decoding iterations. The investigation of the impact of iterative detection-decoding or iterative scheduling on the performance is still pending and not yet presented. The turbo decoder performs up to 6 internal iterations. The size of a transport block $\mathbf{u}_t$ is 1600 bits, composing one frame. For the sake of clarity the two-stage and single-stage schemes are denoted by *FDE-TSD* and *FDE*, respectively.

Comparing non-iterative (*#It*=0) FDE and FDE-TSD at the 10^{-1} target FER, a performance gain of 6.3 dB and 3.3 dB is observed for the low-ISI and high-ISI scenario, respectively. When FDE-TSD carries out additional equalization-decoding iterations, the performance further increases by up to 1.0 dB and 2.5 dB, respectively. Since IAI is the dominating interference in the low-ISI scenario, FDE-TSD outperforms FDE due to the powerful sphere detection, even if iterations are carried out. As soon as channels with significant ISI are considered, the impact of the sphere detector on the overall performance result decreases. This leads to a lower gain in the non-iterative, but to higher gains in the iterative case. In the low SNR regime, when noise becomes the critical factor, FDE seems to outperform FDE-TSD. The reason is that the sphere detector performs rather non-optimal soft-demodulation in contrast to the 4 ideal soft-demodulators deployed in the single-stage approach. An ideal soft-demodulator exhibits very high complexity, making it difficult to fairly compare both approaches. Note that if $h'[3]$ (most dominant channel tap in the high-ISI scenario) instead of $h'[1]$ would be selected as target channel tap, an even better FER performance could be observed.

A. Stop Criterion and Iteration Complexity Analysis

In iterative receivers, a received signal is processed multiple times before a final estimate is determined. This increases the computational complexity linearly with the number of external iterations. Since especially in the high SNR regime additional receiving processing loops may not lead to a more reliable estimate, a stop criterion is introduced to avoid unnecessary iteration runs. For this purpose, the cyclic redundancy check (CRC) of all T turbo decoders is analyzed. Only if all CRCs are correct, the iterative processing stops. Otherwise another iterative run for an already processed transport block is started, unless the maximum number of equalization-decoding iterations *max. #It* is reached.

This stop criterion and its effect on the iteration complexity is analyzed in Fig. 5, depicting the averaged relative number of receiver runs in each iterations for the FDE-TSD. At the SNR values corresponding to the target FER of 10^{-1}, the first iteration loop *It=1* is only carried out in 34 % (low-ISI scenario) and 69 % (high-ISI scenario) of the cases. The second iteration loop *It=2* is carried out in 21 % (low-ISI scenario) and 33 % (high-ISI scenario) of the cases. If we would restrict the maximum number of iterations *max. #It* to 1, a performance gain of 0.9 dB(1.9 dB) could be observed while the complexity increases by 31 %(59 %) for the low-ISI (high-ISI) scenario.

Although the computation costs in practical implementations are decreased on average, the CRC decisions vary the number of iterations and therefore affect the processing steps for each received frame of SC-FDMA symbols. From a system level perspective, this imposes high requirements on heterogeneous software defined radio platforms in terms of dynamic task scheduling and fast allocation of processing elements [15].

VI. Conclusion

Throughout this work, a two-stage scheme, combining frequency-domain equalization with time-domain sphere detection, has been developed and deployed in a multi-iterative receiver. The error-rate performance of the proposed scheme

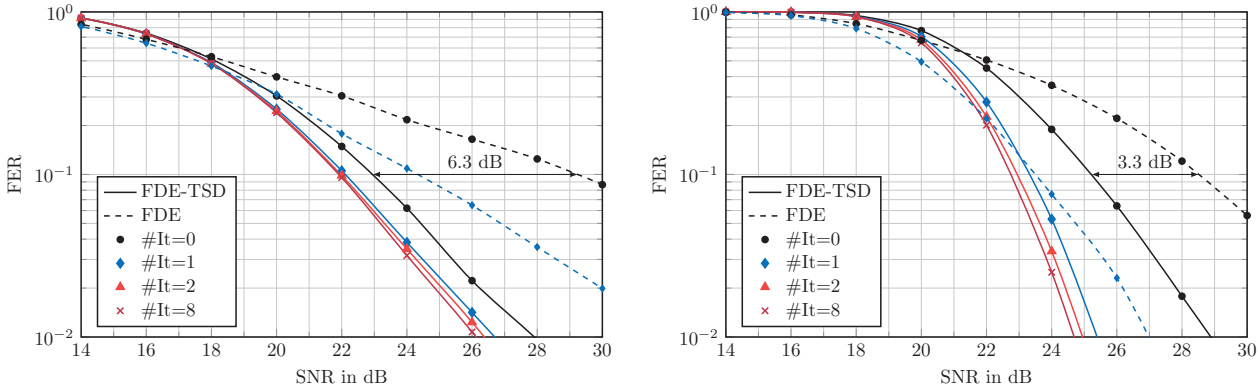

(a) EPA delay profile, 1.4 MHz user bandwidth (72 subcarriers)

(b) ETU delay profile, 5.0 MHz user bandwidth (300 subcarriers)

Fig. 4. FER performance comparison between SISO single-stage (FDE) and SISO two-stage (FDE-TSD) scheme for the LTE-A uplink 4×4 MIMO channel with CQI=10 (64-QAM, code rate $\rho = 0.45$). The size of transport block $\mathbf{u}_t$ is 1600 bits, composing one frame. The turbo decoder performs up to 6 internal iterations. The SNR is defined by σ_x^2/σ_n^2.

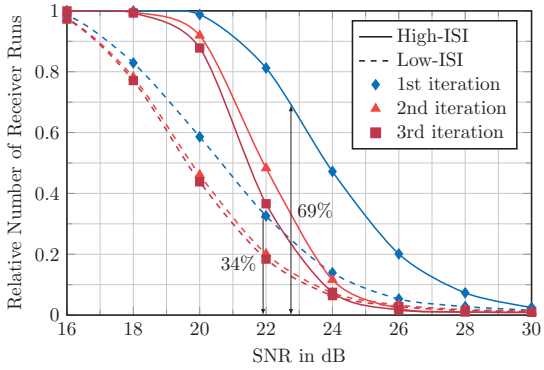

Fig. 5. Iteration complexity analysis of FDE-TSD, *max. #It=8*: Relative number of receiver runs is depicted for each individual loop (1st iteration, 2nd iteration, etc.). The vertical arrows indicate the SNR value to achieve an FER of 10^{-1}. For example, observing the high-ISI scenario at SNR $= 26$ dB, the first iteration is carried out for 20 % of the received frames on average.

has been investigated for an LTE-A uplink setup in consideration of different ISI scenarios. As shown by the performance results, the two-stage approach outperforms the conventional single-stage approach, especially when antenna-interference dominates the overall interference. Performing additional equalization-decoding iterations, which is mainly focusing on ISI cancellation, can further increase the performance even for low-ISI channels. Throughout this work it has been thus demonstrated that such a multi-stage multi-iterative receiver enables adaptable processing with respect to the dominating interferences.

This work has been supported by the German Federal Ministry of Education and Research within the program "Twenty20" under contract 03ZZ0505B - "fast wireless" and by the German Research Foundation in the framework of priority program SPP 1655 "Wireless Ultra High Data Rate Communication for Mobile Internet Access". Computations were performed on a PC-Cluster at the Center for Information Services and High Performance Computing (ZIH) at TU Dresden.

References

[1] 3GPP, "Feasibility study for Further Advancements for E-UTRA (LTE-Advanced)," 3rd Generation Partnership Project (3GPP), TR 36.912, Mar. 2011.

[2] B. Mennenga, A. von Borany, and G. Fettweis, "Complexity reduced Soft-In Soft-Out Sphere Detection based on Search Tuples," in *Proc. IEEE Int. Conf. Commun. (ICC'09)*, Dresden, Germany, Jun. 2009, pp. 1–6.

[3] C. Studer and H. Bolcskei, "Soft-Input Soft-Output Single Tree-Search Sphere Decoding," *IEEE Trans. Inf. Theory*, vol. 56, no. 10, pp. 4827–4842, Oct. 2010.

[4] E. P. Adeva, T. Seifert, and G. Fettweis, "VLSI Architecture for MIMO Soft-Input Soft-Output Sphere Detection," *J. Signal Process. Syst.*, vol. 70, no. 2, pp. 125–143, 2013.

[5] E. M. Witte, F. Borlenghi, G. Ascheid, R. Leupers, and H. Meyr, "A Scalable VLSI Architecture for Soft-Input Soft-Output Single Tree-Search Sphere Decoding," *IEEE Trans. Circuits Syst. II, Exp. Briefs*, vol. 57, no. 9, pp. 706–710, Sep. 2010.

[6] J. Ketonen, J. Karjalainen, M. Juntti, and T. Hänninen, "MIMO Detection in Single Carrier Systems," in *Proc. Eur. Signal Process. Conf.*, 2011, pp. 654–658.

[7] M. Tüchler and A. Singer, "Turbo Equalization: An Overview," *IEEE Trans. Inf. Theory*, vol. 57, no. 2, pp. 920–952, Feb. 2011.

[8] N. Benvenuto, R. Dinis, D. Falconer, and S. Tomasin, "Single Carrier Modulation With Nonlinear Frequency Domain Equalization: An Idea Whose Time Has Come Again," *Proc. IEEE*, vol. 98, no. 1, pp. 69–96, 2010.

[9] T. Seifert and G. Fettweis, "Soft-PIC Frequency-Domain Equalization in Iterative MIMO Receivers for the LTE-A Uplink," in *Proc. IEEE 79th Veh. Technol. Conf.*, May 2014, pp. 1–5.

[10] A. Czylwik, "Comparison between adaptive OFDM and single carrier modulation with frequency domain equalization," in *Proc. IEEE 47th Veh. Technol. Conf.*, vol. 2, 1997, pp. 865–869.

[11] J. Proakis and D. Manolakis, *Digital Signal Processing (4th Edition)*. Prentice Hall, 2006.

[12] J. Hagenauer, "The Turbo Principal in Mobile Communications," in *Proc. Int. Symp. Inf. Theory and Appl. (ISITA'02)*, Xi'an, China, Oct. 2002.

[13] M. Tüchler, A. Singer, and R. Koetter, "Minimum mean squared error equalization using a priori information," *IEEE Trans. Signal Process.*, vol. 50, no. 3, pp. 673–683, Mar. 2002.

[14] B. Mennenga and G. Fettweis, "Search Sequence Determination for Tree Search based Detection Algorithms," in *Proc. IEEE Sarnoff Symp.*, Princeton, USA, Mar. 2009, pp. 1–6.

[15] B. Noethen *et al.*, "10.7 A 105GOPS 36mm2 heterogeneous SDR MPSoC with energy-aware dynamic scheduling and iterative detection-decoding for 4G in 65nm CMOS," in *IEEE Int. Solid-State Circuits Conf. Dig. Tech. Papers (ISSCC'14)*, Feb. 2014, pp. 188–189.